Preparation of Entangled States through Hilbert Space Engineering

Y. Lin,[1,*] J. P. Gaebler,[1] F. Reiter,[2,†] T. R. Tan,[1] R. Bowler,[1,‡] Y. Wan,[1] A. Keith,[1] E. Knill,[1] S. Glancy,[1] K. Coakley,[1] A. S. Sørensen,[2] D. Leibfried,[1] and D. J. Wineland[1]

[1]*National Institute of Standards and Technology, 325 Broadway, Boulder, Colorado 80305, USA*

[2]*The Niels Bohr Institute, University of Copenhagen, Blegdamsvej 17, DK-2100 Copenhagen Ø, Denmark*

(Received 15 June 2016; published 28 September 2016)

We apply laser fields to trapped atomic ions to constrain the quantum dynamics from a simultaneously applied global microwave field to an initial product state and a target entangled state. This approach comes under what has become known in the literature as "quantum Zeno dynamics" and we use it to prepare entangled states of two and three ions. With two trapped $^9Be^+$ ions, we obtain Bell state fidelities up to 0.990^{+2}_{-5}; with three ions, a W-state fidelity of 0.910^{+4}_{-7} is obtained. Compared to other methods of producing entanglement in trapped ions, this procedure can be relatively insensitive to certain imperfections such as fluctuations in laser intensity.

DOI: 10.1103/PhysRevLett.117.140502

The quantum Zeno effect has historically referred to the inhibition of quantum dynamics due to frequent measurements [1–3]. More generally, the idea is to restrict the dynamics to a subspace of the overall system. Recent theoretical proposals [4–11] have explored ways to provide this subspace isolation by coupling the remainder of the system to auxiliary quantum states. This situation has become known as quantum Zeno dynamics [12–14], even though the restrictions can be implemented by unitary interactions without the need for measurements. Dynamics in a restricted subspace have recently been demonstrated with atoms in Bose-Einstein condensates [15], Rydberg atoms [16,17], atoms in a cavity [18], and photons in a cavity coupled to a superconducting qubit [19]. Here, we apply coherent laser fields to trapped ions which couple some of their combined internal (hyperfine) states to a mechanical mode of their motion. These states are perturbed (dressed) in such a way that when applying an additional (microwave) field, the dynamics are restricted to the states not coupled by the laser fields. Under suitable conditions, only two states are coupled by the microwaves: a separable (product) state and an entangled state. With this Hilbert space engineering, we can therefore prepare an entangled state by applying a spatially uniform microwave field to a collection of ions initially in a separable state. For measurement-based Zeno dynamics, there is a finite probability of irretrievably escaping from the desired subspace. However, if the subspace restriction is brought about by coherent interactions, the evolution is ideally unitary, and thus state amplitudes that leak from the restricted subspace remain coherent and can be recovered with additional coherent operations. We demonstrate this advantage of coherent subspace engineering by applying a composite pulse sequence, and observe an improved fidelity of the entangled state. Also, the technique described here can produce entangled states with resilience to laser intensity noise when compared to the laser-based deterministic entangling operations typically used in trapped ion experiments.

When applying a global rotation to an initial state with N two-level (spin-$\frac{1}{2}$) systems in the spin up state $|\uparrow\rangle$, each spin rotates independently and the overall quantum state remains separable. The evolution can be described in the symmetric angular momentum manifold $|J = N/2, m_J\rangle$ [20], or Dicke states [21], where J is the total angular momentum quantum number and m_J is the projection of the angular momentum along the quantization axis. All individual $|J, m_J\rangle$ states are entangled states except the maximal spin states, $|\uparrow\uparrow\ldots\uparrow\rangle = |J, J\rangle$ and $|\downarrow\downarrow\ldots\downarrow\rangle = |J, -J\rangle$. Entanglement between multiple spins can be generated by perturbing specific $|J, m_J\rangle$ states in the manifold to restrict the dynamics. A simple case is to apply a perturbation to shift the $|J, J-2\rangle$ state out of resonance, as depicted in Fig. 1 for the case of two spins. In this case, the dynamics are restricted within the $|J, J\rangle$ and $|J, J-1\rangle$ states. Thus, starting from $|J, J\rangle$, the entangled $|J, J-1\rangle$ state is prepared by an effective π pulse. For two and three spins, these states are the triplet Bell state $|T\rangle = (1/\sqrt{2})(|\uparrow\downarrow\rangle + |\downarrow\uparrow\rangle)$ and the W state [22] $|W\rangle = (1/\sqrt{3})(|\uparrow\uparrow\downarrow\rangle + |\uparrow\downarrow\uparrow\rangle + |\downarrow\uparrow\uparrow\rangle)$, respectively.

We experimentally demonstrate this scheme with trapped $^9Be^+$ ions aligned along the axis of a linear Paul trap [23–25]. In an applied magnetic field of 11.946 mT, the frequency splitting $\omega_0 \approx 2\pi \times 1.2075$ GHz between the $^2S_{1/2}$ hyperfine ground states $|F = 2, m_F = 0\rangle \equiv |\downarrow\rangle$ and $|F = 1, m_F = 1\rangle \equiv |\uparrow\rangle$ is first-order insensitive to magnetic field fluctuations [26]. These two states represent the spin-1/2 system, or qubit, in the experiment. The effective rotation in the restricted subspace is produced by a uniform resonant microwave field, while the Hilbert space restricting perturbations are provided by a laser-induced coupling between ions via a shared motional mode. With two ions

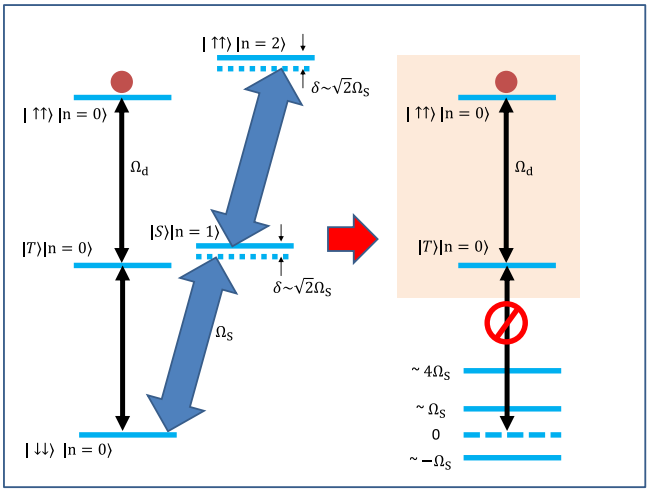

FIG. 1. Restricted dynamics for two ions. The thin black arrows depict the relatively weak microwave coupling; the thick blue arrows depict laser-induced strong blue sideband coupling. With the $|\uparrow\uparrow\rangle$ state initially populated (red dots), in the absence of the sideband excitation, the microwaves drive the state down the symmetric manifold (the states on the left) with Rabi frequency Ω_d, where the $|T\rangle$ and $|S\rangle$ states are defined in the text, and such a global rotation alone cannot generate entanglement. However, the sideband excitations (with Rabi frequency Ω_s) dress the $|\downarrow\downarrow\rangle$ state, shifting its components out of resonance with respect to the weak microwave drive, as shown on the right. Thus given $\Omega_s \gg \Omega_d$, the microwave drive only couples the two highest energy states in the symmetric manifold, and the entangled $|T\rangle$ state can be created with an effective π pulse of the microwave drive ($t_\pi = \pi/(2\sqrt{2}\Omega_d)$) from the $|\uparrow\uparrow\rangle$ state.

and without applied laser fields, the microwave field couples the Dicke states with the Hamiltonian

$$H_d = \hbar\Omega_d \sum_{i=1,2} \sigma_i^x = \sqrt{2}\hbar\Omega_d(|\downarrow\downarrow\rangle\langle T| + |T\rangle\langle\uparrow\uparrow|) + \text{H.c.},$$

where $\hbar$ is the reduced Planck constant, Ω_d is the single-ion Rabi frequency, σ_i^x is the Pauli operator on the ith ion, and H.c. stands for Hermitian conjugate. If the spins are initially in a product state, evolution under this Hamiltonian will not generate entanglement.

To generate the desired dynamics for two ions, we address the "stretch" axial normal mode of motion of frequency $\omega \approx 2\pi \times 6.20$ MHz, with a laser-induced stimulated-Raman blue sideband interaction [27]. The sideband interaction is detuned from resonance by δ, and is described by the Hamiltonian

$$H_s = \hbar\Omega_s(\sigma_1^- - \sigma_2^-)ae^{-i\delta t} + \text{H.c.}, \qquad (2)$$

where Ω_s is the Rabi frequency, a is the annihilation operator of the stretch mode, and $\sigma_i^- = |\downarrow\rangle_i\langle\uparrow|$ is the spin lowering operator for ion i. In Eq. (2), we have assumed that the Raman phase on the two ions is the same (modulo 2π). The minus sign between the two spin lowering operators results from the stretch-mode amplitudes being equal but opposite sign for the two ions. The symmetry of the $|T, n\rangle$ state implies that the sideband interaction does not couple this state to other relevant states. However, as depicted on the left in Fig. 1, it couples the states $|\downarrow\downarrow\rangle|n\rangle \leftrightarrow |S\rangle|n+1\rangle \leftrightarrow |\uparrow\uparrow\rangle|n+2\rangle$, where $|n\rangle$ denotes a stretch mode Fock state, and $|S\rangle = (1/\sqrt{2})(|\uparrow\downarrow\rangle - |\downarrow\uparrow\rangle)$. The energies of the resulting dressed states (the eigenstates of the ions with H_s included) are shifted to approximately $\pm\hbar\Omega_s$ and $4\hbar\Omega_s$ (right-hand side of Fig. 1), when the detuning δ is set to approximately $\sqrt{2}\Omega_s$ [27], so that the energy shift can be made large compared to $\hbar\Omega_d$ for $\Omega_s \gg \Omega_d$. In addition, H_s couples $|\uparrow\uparrow, n\rangle$ to $|S, n-1\rangle$ for $n > 0$, but these couplings are absent if we initialize the stretch mode in the ground state $n = 0$. If $\Omega_s \gg \Omega_d$, the system evolves as an effective two-level system between $|\uparrow\uparrow\rangle|0\rangle$ and $|T\rangle|0\rangle$ under the combined influence of H_s and H_d, within a subspace isolated from other states. This allows the preparation of the entangled state $|T\rangle|0\rangle$ by a single effective π pulse from $|\uparrow\uparrow\rangle|0\rangle$. However, for $n > 0$, the desired subspace will not be isolated; therefore, high fidelity motional ground state preparation is crucial [27].

To initialize the spin and motional states, we first sideband cool both axial modes of the ions to near the ground state, achieving average motional occupation of $\bar{n} < 0.006$ for the stretch mode [38]. Optical pumping prepares both ions in the $|F = 2, m_F = 2\rangle$ atomic state. We then apply a global composite microwave π pulse to initialize to the $|\uparrow\uparrow\rangle$ state [27,39]. We set the laser beam and microwave intensities to give $\Omega_s \approx 2\pi \times 17.6$ kHz and $\Omega_d \approx 2\pi \times 1.52$ kHz. We choose $\delta \approx 2\pi \times 27.1$ kHz while maintaining a Raman detuning of approximately $2\pi \times 480$ GHz red detuned from the $^2P_{1/2}$ state. We simultaneously apply microwaves and laser beams for a variable duration t, followed by detection pulses. We observe coherent Rabi flopping between the $|\uparrow\uparrow\rangle$ and $|T\rangle$ states as shown in Fig. 2, where the population in the $|\uparrow\uparrow\rangle$ and $|\downarrow\downarrow\rangle$ states and the fidelity of the $|T\rangle$ state are determined as described in the Supplemental Material [27].

We observe a maximal fidelity of the $|T\rangle$ state of 0.981^{+2}_{-4} after a duration of $t_\pi \approx 116$ μs, which matches the theoretical prediction [27] of $t_\pi = \pi/(2\sqrt{2}\Omega_d)$. The fidelities and error bars are derived from maximum likelihood partial state tomography, parametric bootstrap resampling, and estimation of state preparation errors [27]. The largest error contributions are estimated to be 0.010 from insufficient isolation of the subspace ($\Omega_s/\Omega_d \approx 12$), 0.008 from spontaneous emission [40], less than 0.006 from imperfect ground state cooling, and less than 0.002 from imperfect initialization of the $|\uparrow\uparrow\rangle$ spin state [27]. We compare our data to a numerical simulation including these errors (solid lines in Fig. 2) and find good agreement. The error from spontaneous emission can be reduced by increasing laser intensity and increasing the detuning of the Raman lasers from the $^2P_{1/2}$ state [41]. The sideband laser beam may

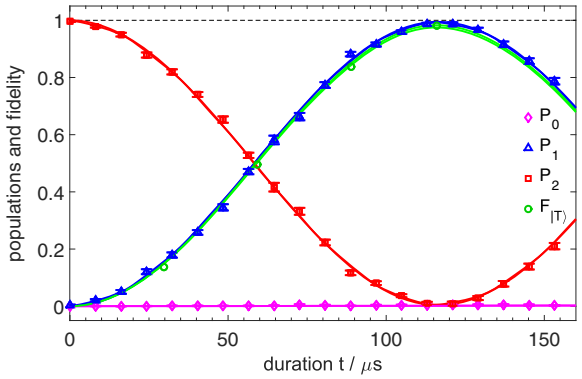

FIG. 2. Two-ion population evolution and $|T\rangle$ state fidelity for restricted dynamics with microwave and sideband excitations applied simultaneously. Population mainly evolves between the $|\uparrow\uparrow\rangle$ and the $|T\rangle$ state, while other states have very small populations. The black dashed line shows unit population and fidelity. The pink diamonds, blue triangles, red squares, and green circles represent the measured populations of states with no spins up P_0, one spin up P_1, two spins up P_2, and the fidelity of the $|T\rangle$ state $F_{|T\rangle}$, respectively. The population measurements are obtained by repeating the experiment 1500 times; the fidelity points are derived from 60 000 experiments [27]. The difference between P_1 and $F_{|T\rangle}$ is due to the population in the $|S\rangle$ state. The solid lines show the results of a numerical simulation taking into account all known experimental imperfections, with the same coloring convention as for the measured populations. We run the simulation with and without including an upper bound on the imperfections of cooling and spin state initialization. The results of these two simulations are indistinguishable on the scale shown in the figure. The populations and fidelity are inferred by means of a maximum likelihood analysis and the error bars represent the uncertainties according to parametric bootstrap resampling [27]. The uncertainties of $F_{|T\rangle}$ are smaller than the symbols.

off-resonantly excite the axial in-phase motional mode (3.6 MHz), causing a small shift ($\approx 0.3\Omega_d$) to the microwave resonance. In our numerical simulations we observe that this effect can be compensated by setting the microwave frequency accordingly and this was incorporated into the experiment by scanning the microwave resonance. One can also adjust the laser polarizations to compensate this shift so that it is laser power independent.

In the absence of spontaneous emission, heating of the motional normal mode and imperfect ground state cooling, the state after the evolution remains a pure state; therefore, any state amplitudes outside the desired subspace can be recovered. To demonstrate this, we apply a specifically tailored composite pulse pair which enables us to return the population in the undesired states $|\downarrow\downarrow, n = 0\rangle$, $|S, n = 1\rangle$, and $|\uparrow\uparrow, n = 2\rangle$ into the isolated subspace and thereby increase the population of $|T\rangle$. To do this we split the laser pulse into two segments of duration t_1 and t_2, changing the laser phase by π and the sideband detuning from δ_1 to $\delta_2 = -\delta_1$. States outside the desired subspace are driven nonresonantly from the $|T\rangle$ state. The amplitudes of these undesired states get a contribution from each of the two pulse segments, leading to an interference between the two contributions, reminiscent of the two-pulse interference in Ramsey spectroscopy. Within first order perturbation theory one can show that the amplitudes of all undesired states interfere destructively and vanish at the time where the fidelity of $|T\rangle$ is maximal if one sets $\delta_1 = -\delta_2 = \sqrt{7/3}\Omega_s$, $\Omega_d = \Omega_s/(3\sqrt{6})$, and $t_2 = 2t_1$. When the amplitudes of the undesired states vanish, the associated constructive interference is in the amplitude of the $|T\rangle$ state which will have a near unity population only limited by higher-order effects [27]. Experimentally we set $\Omega_s = 2\pi \times 17.3$ kHz, $\Omega_d = 2\pi \times 2.55$ kHz, $\delta_1 = -\delta_2 = 2\pi \times 26.8$ kHz, $t_1 = 25.4$ μs, and $t_2 = 47.3$ μs to obtain a $|T\rangle$ state population of 0.990^{+2}_{-5}. The symbols in Fig. 3 show the experimentally observed population evolution during the composite pulse sequence, in agreement with numerical simulations (solid lines). Higher fidelity is achieved despite a smaller ratio $\Omega_s/\Omega_d \approx 7$, by recovering amplitudes that leaked out due to insufficient isolation of the subspace, reducing this error to 0.001. (We note that according to simulations, further reduction can be achieved with better calibration of t_1.) The reduced Ω_s/Ω_d has the beneficial effect of suppressing the spontaneous emission error to 0.005. Similar to the single-pulse experiment, we estimate errors less than 0.005 from imperfect ground state cooling, and less than 0.002 from imperfect initialization of the $|\uparrow\uparrow\rangle$ spin state [27]. We compare our data to a

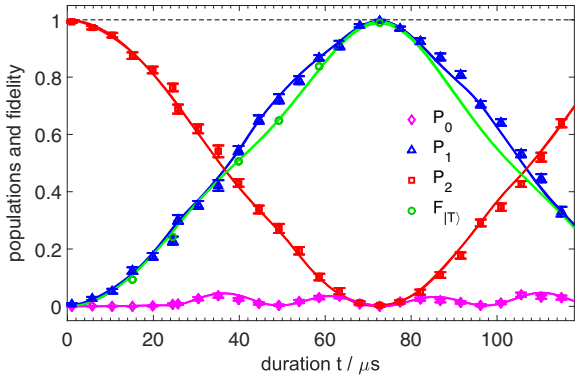

FIG. 3. State evolution for restricted dynamics of two trapped ions using a composite pulse sequence. Similar to Fig. 2, populations are mainly confined to the $|\uparrow\uparrow\rangle$ and $|T\rangle$ states. The coloring and labeling conventions are the same as in Fig. 2. The laser beam phase and detuning are flipped 25.4 μs after the start of the experiment. Note that the oscillations of $|\downarrow\downarrow\rangle$ are enhanced for $t > 25.4$ μs; however, the maximal population of the $|T\rangle$ state is increased compared to the single pulse used for the data in Fig. 2. We numerically simulate this experiment with and without including an upper bound of imperfections of cooling and spin state initialization. The simulation results overlap on the scale of the figure. The populations, fidelity, and error bars are inferred as in Fig. 2 [27]. The population measurements are obtained by repeating the experiment 1000 times; the fidelity points are derived from 40 000 experiments [27]. The uncertainties of $F_{|T\rangle}$ are smaller than the symbols.

numerical simulation including these errors (solid lines in Fig. 3) and find good agreement.

We also demonstrate restricted dynamics on three $^9Be^+$ ions. We tune the laser beam frequencies to address the center-of-mass (c.m.) mode blue sideband, which has equal mode amplitudes on each ion. The ion spacings are set such that the phase of the sideband interaction on each ion differs by $2\pi/3$ so that the $|W, n = 0\rangle$ state will be a dark state of the sideband interaction [27]. Starting from the $|\uparrow\uparrow\uparrow, n = 0\rangle$ state, and with driving field parameters similar to the case of two ions, we observe flopping between the $|\uparrow\uparrow\uparrow\rangle$ and $|W\rangle$ states, shown in Fig. 4 and in agreement with the numerical simulations [27]. We obtain a $|W\rangle$ state fidelity of 0.910^{+4}_{-7} after a duration of 114.1 μs, as shown in Fig. 4. The sources of infidelity include those of the two-ion case (in general leading to larger imperfections) plus two sizable additions: 0.011 from heating of the c.m. mode caused by electric field noise and 0.023 from unequal laser illumination on the three ions due to the Gaussian profile of the laser beam [27].

For more than three ions in a chain, numerical simulations and analytic analysis indicate the presence of unwanted dark states such that straightforward application of the sideband interaction does not yield an effective two-level system between the first two Dicke states. However, by using a sideband coupling to an auxiliary level, the scheme can be scaled up to multiple spins [42].

In summary, we describe and demonstrate a scheme to isolate subspaces of spin states with trapped ions, enabling the creation of entangled states by the application of global uniform oscillating fields. We create a two-ion triplet Bell state with fidelity of 0.990^{+2}_{-5}, and a three-ion $|W\rangle$ state with fidelity of 0.910^{+4}_{-7}. By reducing spontaneous emission [40] and increasing the initial ground state preparation fidelity, the overall fidelities of the $|T\rangle$ and $|W\rangle$ states can be improved.

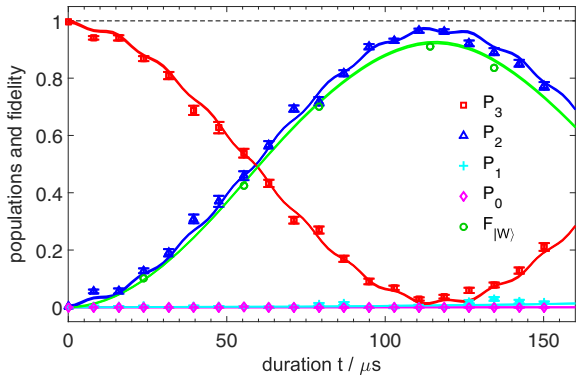

FIG. 4. Population evolution for three ions. The red squares, blue triangles, cyan crosses, pink diamonds, and green circles represent the measured probabilities of three spins up, two, one, and no spin up and the fidelity of the $|W\rangle$ state, denoted as P_i (i = 3-0) and $F_{|W\rangle}$, respectively. Solid lines are the result of the numerical simulation, with and without the imperfection of spin state initialization. The simulation results are overlapping on the scale shown in the figure. The population measurements are obtained by repeating the experiment 1000 times, and for the fidelity measurements we take additional data, as described in the Supplemental Material [27]. The uncertainties of $F_{|W\rangle}$ are smaller than the labels.

At the current state of trapped ion technology, this technique cannot compete with the best entangling gates [41,43]. However, under certain conditions, the entangled state fidelity resulting from subspace engineering is relatively insensitive to fluctuations in laser intensity, since the main requirement is that the frequency shifts due to the laser-induced spin-motion coupling are large compared to the microwave Rabi frequency, but the exact value and stability of the shifts are not crucial [27]. Furthermore, for some laser-based gates, the phase of the entangled states depends directly on the phase(s) of the laser beam(s) at the site of the ions. This phase can depend on beam path fluctuations, such as those caused by air currents. For the technique described here, laser beam phase does not play a role, since the entangled state phase is controlled by microwaves which are highly immune to such effects. A fundamental limitation on fidelity for our technique is the requirement for ground state cooling; however, as the field advances, it is likely that ground-state cooling will also improve. Therefore, this scheme may serve as an alternative way of preparing entangled states, without using conventional multiqubit entangling quantum logic gates [44]. This work also presents an application of Hilbert space engineering, which may be extended to generate other entangled states or spin dynamics. Our scheme can be generalized to other experimental platforms, for example, superconducting qubits or atoms in a cavity.

We thank J. Eschner, G. Morigi, and A. Signoles for helpful discussions. We thank C. Kurz and D. H. Slichter for helpful comments on the manuscript. The NIST work was supported by the Office of the Director of National Intelligence (ODNI) Intelligence Advanced Research Projects Activity (IARPA), ONR, and the NIST Quantum Information Program. The work of the University of Copenhangen was funded by the European Union Seventh Framework Programme through ERC Grant QIOS (Grant No. 306576).

This paper is a contribution by NIST and not subject to U.S. copyright.

*To whom correspondence should be addressed.
yiheng.lin@colorado.edu
Present address: JILA, National Institute of Standards and Technology and University of Colorado, and Department of Physics, University of Colorado, Boulder, CO 80309, USA.
†Present address: Harvard University, Department of Physics, 17 Oxford Street, Cambridge, MA 02138, USA.

[‡]Present address: University of Washington, Department of Physics, Box 351560, Seattle, Washington 98195, USA.

[1] B. Misra and E. C. G. Sudarshan, J. Math. Phys. (N.Y.) **18**, 756 (1977).
[2] W. M. Itano, D. J. Heinzen, J. J. Bollinger, and D. J. Wineland, Phys. Rev. A **41**, 2295 (1990).
[3] C. Balzer, T. Hannemann, D. Reiß, C. Wunderlich, W. Neuhauser, and P. E. Toschek, Opt. Commun. **211**, 235 (2002).
[4] S. Maniscalco, F. Francica, R. L. Zaffino, N. Lo Gullo, and F. Plastina, Phys. Rev. Lett. **100**, 090503 (2008).
[5] X.-B. Wang, J. Q. You, and F. Nori, Phys. Rev. A **77**, 062339 (2008).
[6] J.-M. Raimond, C. Sayrin, S. Gleyzes, I. Dotsenko, M. Brune, S. Haroche, P. Facchi, and S. Pascazio, Phys. Rev. Lett. **105**, 213601 (2010).
[7] A. Smerzi, Phys. Rev. Lett. **109**, 150410 (2012).
[8] D. Burgarth, P. Facchi, V. Giovannetti, H. Nakazato, S. Pascazio, and K. Yuasa, Phys. Rev. A **88**, 042107 (2013).
[9] Y. Li, D. A. Herrera-Martí, and L. C. Kwek, Phys. Rev. A **88**, 042321 (2013).
[10] B. Zhu, B. Gadway, M. Foss-Feig, J. Schachenmayer, M. L. Wall, K. R. A. Hazzard, B. Yan, S. A. Moses, J. P. Covey, D. S. Jin, J. Ye, M. Holland, and A. M. Rey, Phys. Rev. Lett. **112**, 070404 (2014).
[11] Y.-R. Zhang and H. Fan, Sci. Rep. **5**, 11509 (2015).
[12] V. Frerichs and A. Schenzle, Phys. Rev. A **44**, 1962 (1991).
[13] P. Facchi and S. Pascazio, Phys. Rev. Lett. **89**, 080401 (2002).
[14] P. Facchi and S. Pascazio, J. Phys. A **41**, 493001 (2008).
[15] F. Schäfer, I. Herrera, S. Cherukattil, C. Lovecchio, F. S. Cataliotti, F. Caruso, and A. Smerzi, Nat. Commun. **5**, 3194 (2014).
[16] A. Signoles, A. Facon, D. Grosso, I. Dotsenko, S. Haroche, J.-M. Raimond, M. Brune, and S. Gleyzes, Nat. Phys. **10**, 715 (2014).
[17] Y.-Y. Jau, A. M. Hankin, T. Keating, I. H. Deutsch, and G. W. Biedermann, Nat. Phys. **12**, 71 (2016).
[18] G. Barontini, L. Hohmann, F. Haas, J. Estève, and J. Reichel, Science **349**, 1317 (2015).
[19] L. Bretheau, P. Campagne-Ibarcq, E. Flurin, F. Mallet, and B. Huard, Science **348**, 776 (2015).
[20] F. T. Arecchi, E. Courtens, R. Gilmore, and H. Thomas, Phys. Rev. A **6**, 2211 (1972).
[21] R. H. Dicke, Phys. Rev. **93**, 99 (1954).
[22] W. Dür, G. Vidal, and J. I. Cirac, Phys. Rev. A **62**, 062314 (2000).
[23] J. Drees and W. Paul, Zeitschrift. für Physik **180**, 340 (1964).
[24] M. G. Raizen, J. M. Gilligan, J. C. Bergquist, W. M. Itano, and D. J. Wineland, Phys. Rev. A **45**, 6493 (1992).
[25] R. B. Blakestad, C. Ospelkaus, A. P. VanDevender, J. M. Amini, J. Britton, D. Leibfried, and D. J. Wineland, Phys. Rev. Lett. **102**, 153002 (2009).
[26] C. Langer, R. Ozeri, J. D. Jost, J. Chiaverini, B. DeMarco, A. Ben-Kish, R. B. Blakestad, J. Britton, D. B. Hume, W. M. Itano, D. Leibfried, R. Reichle, T. Rosenband, T. Schaetz, P. O. Schmidt, and D. J. Wineland, Phys. Rev. Lett. **95**, 060502 (2005).
[27] See Supplemental Material at http://link.aps.org/supplemental/10.1103/PhysRevLett.117.140502, for which includes Refs. [28-37].
[28] D. J. Wineland, C. Monroe, W. M. Itano, D. Leibfried, B. E. King, and D. M. Meekhof, J. Res. Natl. Inst. Stand. Technol. **103**, 259 (1998).
[29] Z. Hradil, J. Řeháček, J. Fiurášek, and M. Ježek, in *Quantum State Estimation* (Springer, Berlin, 2004).
[30] B. Efron and R. J. Tibshirani, *An Introduction to the Bootstrap* (Chapman & Hall, Boca Raton, 1993).
[31] J. Oosterhoff and W. R. van Zwet, in *Proceedings of the Sixth Berkeley Symposium on Mathematical Statistics and Probability*, Vol. 1 (University of California Press, 1972), pp. 31–50.
[32] D. D. Boos, Stat. Sci. **18**, 168 (2003).
[33] E. L. Hahn, Phys. Rev. **80**, 580 (1950).
[34] C. Ospelkaus, U. Warring, Y. Colombe, K. R. Brown, J. M. Amini, D. Leibfried, and D. J. Wineland, Nature (London) **476**, 181 (2011).
[35] N. Timoney, I. Baumgart, M. Johanning, A. F. Varón, M. B. Plenio, A. Retzker, and C. Wunderlich, Nature (London) **476**, 185 (2011).
[36] A. Sørensen and K. Mølmer, Phys. Rev. Lett. **82**, 1971 (1999).
[37] A. Sørensen and K. Mølmer, Phys. Rev. A **62**, 022311 (2000).
[38] C. Monroe, D. M. Meekhof, B. E. King, S. R. Jefferts, W. M. Itano, D. J. Wineland, and P. Gould, Phys. Rev. Lett. **75**, 4011 (1995).
[39] M. H. Levitt, Prog. Nucl. Magn. Reson. Spectrosc. **18**, 61 (1986).
[40] R. Ozeri, W. M. Itano, R. B. Blakestad, J. Britton, J. Chiaverini, J. D. Jost, C. Langer, D. Leibfried, R. Reichle, S. Seidelin, J. H. Wesenberg, and D. J. Wineland, Phys. Rev. A **75**, 042329 (2007).
[41] J. P. Gaebler, T. R. Tan, Y. Lin, Y. Wan, R. Bowler, A. C. Keith, S. Glancy, K. Coakley, E. Knill, D. Leibfried, and D. J. Wineland, Phys. Rev. Lett. **117**, 060505 (2016).
[42] F. Reiter *et al.* (work in progress).
[43] C. J. Ballance, T. P. Harty, N. M. Linke, M. A. Sepiol, and D. M. Lucas, Phys. Rev. Lett. **117**, 060504 (2016).
[44] H. Häffner, W. Hänsel, C. F. Roos, J. Benhelm, D. Chek-al-kar, M. Chwalla, T. Körber, U. D. Rapol, M. Riebe, P. O. Schmidt, C. Becher, O. Gühne, W. Dür, and R. Blatt, Nature (London) **438**, 643 (2005).